Science of the Total Environment 800 (2021) 149494

Contents lists available at ScienceDirect

Science of the Total Environment

journal homepage: www.elsevier.com/locate/scitotenv

Changes in floodplain hydrology following serial damming of the Tocantins River in the eastern Amazon

A. Christine Swanson [a,*], David Kaplan [b], Kok-Ben Toh [c], Elineide E. Marques [d], Stephanie A. Bohlman [a]

[a] School of Forest, Fisheries, and Geomatics Sciences, University of Florida, 1745 McCarty Dr., Gainesville, FL 32611, United States of America
[b] Department of Environmental and Engineering Sciences, University of Florida, 102 Phelps Lab, Gainesville, FL 32611, United States of America
[c] School of Natural Resources and Environment, University of Florida, 1745 McCarty Dr., Gainesville, FL 32611, United States of America
[d] Graduate Program in Environmental Science (PPGCiamb), Department of Biology, Federal University of Tocantins, Avenida NS 15, Quadra 109 Norte, Complexo Lamadrid, Palmas, TO 77001-090, Brazil

HIGHLIGHTS

- Amazonian rivers are under increasing pressure for hydropower production.
- The Tocantins River has the highest number of dams in Amazon.
- Measured and modeled changes in floodplain inundation after damming
- Flood extent and hydroperiod decreased and flood initiation delayed after damming
- Cascade dams alter hydrology and disconnect Amazonian rivers and their floodplains.

GRAPHICAL ABSTRACT

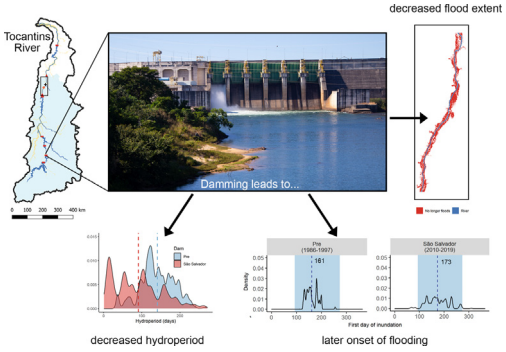

ARTICLE INFO

Article history:
Received 2 June 2021
Received in revised form 30 July 2021
Accepted 2 August 2021
Available online 5 August 2021

Editor: Fernando A.L. Pacheco

Keywords:
Hydro-electric dams
Dam complexes
Floodplain modeling
Cerrado
Brazil
Agência Nacional das Águas (ANA)

ABSTRACT

Riparian forests are ecotones that link aquatic and terrestrial habitats, providing ecosystem services including sediment control and nutrient regulation. Riparian forest function is intimately linked to river hydrology and floodplain dynamics, which can be severely altered by dams. The Tocantins River in the eastern Amazon has six mega-dams along its course. To understand the large-scale and cumulative impacts of multiple dams on the Tocantins floodplain, we quantified landscape-scale changes in floodplain extent, hydroperiod, and flood timing on a 145-km stretch of the river downstream of five dams. We used water level data from 1985 to 2019 to compare daily floodplain inundation dynamics before and after damming. We also developed models to examine the impacts of climate and land use change on hydrology of the Tocantins River. After installation of the first dam in 1998, an average of 82.3 km^2 (63%) of the floodplain no longer flooded, overall average hydroperiod decreased by 15 days (11%), and flooding started an average of five days earlier. After all five dams were installed, 72% of the average pre-dam flooded area no longer flooded, average hydroperiod had decreased by 35%, and average inundation onset occurred 12 days later. These changes in floodplain hydrology appeared to be driven primarily by dam operations as we found no significant changes in precipitation over the study period. Increasing loss of natural vegetation in the watershed may play a role in changed hydrology but cannot explain the abrupt loss of floodplain extent after the first dam was installed. This is one of few studies to quantify dam-induced floodplain alteration at a landscape scale and to investigate impacts of multiple dams on a landscape. Our results indicate that the Tocantins River floodplain is undergoing drastic hydrologic alteration. The impacts of multiple dams are cumulative and non-linear, especially for hydroperiod and flood timing.

* Corresponding author.
E-mail address: a.christine.swanson@gmail.com (A.C. Swanson).

https://doi.org/10.1016/j.scitotenv.2021.149494

1. Introduction

Floodplains and riparian forests provide important ecosystem services, including nutrient regulation and sediment and erosion control (Naiman et al., 1993). In many parts of the world, they are also essential for subsistence floodplain agriculture (Fox and Ledgerwood, 1999; Junk, 2001). The ecological integrity of riparian forests is especially important in the Amazon basin, which has one of the largest extents of riparian and floodplain forests in the world (Junk, 2010). These extensive forests help support fish biodiversity and maintain fisheries, providing food and shelter to many species during high water periods when the forests are flooded (Saint-Paul et al., 2000; Lobón-Cerviá et al., 2015; Arantes et al., 2018). These forests are also the most species-rich floodplain forests in the world (Wittmann et al., 2010). The function of riparian forest is intimately linked to river hydrology and floodplain dynamics (Junk et al., 1989; Jardine et al., 2015), such that alterations in flow impact the composition and function of these forests.

Riverine flow regime is characterized by five main components: magnitude, frequency, duration, timing, and rate of change (Poff et al., 1997). Changes in each flow regime component can affect riparian ecosystem structure and function (Kozlowski, 2002; Poff and Zimmerman, 2010). For instance, flow stabilization, or decrease in the variation in magnitude, can lead to species invasions, declines in seedling establishment and regeneration, and reduced growth rates for trees (Rood and Mahoney, 1995; Zamora-Arroyo et al., 2001; Shafroth et al., 2002; van Oorschot et al., 2018). Loss of seasonal high flows (timing) can diminish plant growth rates, lead to higher plant mortality (Reily and Johnson, 1982), and also promote invasions of riparian species (Horton, 1977). Prolonged low flow events related to changes in flow (duration) reduce plant cover and decrease plant species diversity (Taylor, 1982). Accelerated flood recession can result in seedlings being unable to establish on the floodplain (Poff et al., 1997). The combination of these flow alterations leads to decreases in riparian species diversity and changes in riparian community composition (Bejarano et al., 2020).

Relationships between river flow and riparian forest structure and function are driven by regular flooding events (Junk et al., 1989). The flood pulse concept posits that the timing and duration of flow in the Amazon and other tropical rivers is key to the maintenance of riparian forest diversity, structure, and function (Junk et al., 1989). For example, riparian forests that undergo rhythmic flood patterns have higher rates of net primary production, compared to those that are subject to more stochastic flooding events (Jardine et al., 2015). Disruption of seasonal flooding due to factors such as extreme drought may cause reduced photosynthetic activity and root respiration, higher seedling mortality, and slower seedling growth rates in riparian forest trees (Parolin et al., 2010). Changes in riparian forest structure and function can lead to bank destabilization and changes in nutrient uptake (Florsheim et al., 2008). Flow alteration also impacts aquatic fauna by disrupting cues for fish spawning and migration and causing loss of access to wetlands and backwater habitats (Welcomme and Halls, 2004).

River flow is ultimately regulated by precipitation and is affected by land cover across the watershed (Poff et al., 1997). Rainfall seasonality controls when high and low flow events occur (Dettinger and Diaz, 2000). Conversion of land cover from natural forest or savanna to urban and agriculture leads to increases in river flow by reducing evapotranspiration (Costa et al., 2003; Dias et al., 2015). As the world's climate changes and large land conversions occur, hydrologic regimes in the world's rivers are being altered (Pokhrel et al., 2018).

In addition to changes in precipitation and land cover, dams drastically alter river hydrology (Magilligan and Nislow, 2005). The largest and most consistent hydrologic changes after damming in the Amazon are related to frequency and duration of high flow events and rate of change of high and low water conditions (Timpe and Kaplan, 2017; Ely et al., 2020). The frequency and duration of high flow events affect how often and how long the floodplain floods. Depending on how they are managed, dams have the capacity to change flooding patterns, including how often an area is flooded, the extent of flooding, and when flooding occurs (Kingsford, 2000; Mumba and Thompson, 2005; Arias et al., 2014). These changes in hydrology may be so extreme as to override flow alterations from climate and land cover change (Timpe and Kaplan, 2017).

Though the Amazon basin is in the midst of a dam-building boom (Lees et al., 2016), there are comparatively few studies of dam impacts on floodplains and riparian ecosystems. Most studies focus at local scales (0.1–10 ha; e.g., Ferreira et al., 2013; da Rocha et al., 2019) or on a single dam (e.g., Manyari and de Carvalho, 2007; Assahira et al., 2017; de Lobo et al., 2019). However, as dam complexes such as the Santo Antônio-Jirau hydro-electric complex in the Madeira basin arise throughout the Amazon, it is imperative to understand how multiple dams across a landscape will affect floodplains and riparian areas.

In this study, we investigated how the construction and operation of multiple dams on a single river have affected the following floodplain hydrology characteristics, specifically: flooding extent, flood duration (hydroperiod), and flood timing. We hypothesized that overall floodplain extent will shrink significantly downstream of the installed dams, but changes will be seasonal, with reduced flooded area in the wet season and increased flooded area during the dry season due to dam operations for energy production. Additionally, we expected that overall hydroperiod would be reduced after damming, and that floods would start later in the year because basin runoff would be held in reservoirs until released for energy needs. With respect to multiple dams, we expected that the first dam on the river would have the greatest impact on flooded extent, hydroperiod, and flood timing, but each additional dam would further decrease flooded extent and hydroperiod. Because we expected the first dam on the river, which is the furthest upstream and only storage dam, to control flow on the river, we did not expect that additional dams would continue to significantly shift flood timing. Finally, we expected that observed changes in floodplain hydrology would be driven primarily by damming rather than climate variation or land cover change.

2. Study site

Our study site is an approximately 145-km stretch of the Tocantins River south (i.e., upstream) of its confluence with the Araguaia River. The study site extends north of the city of Miracema do Tocantins (−9.5591, −48.3798) to south of the city of Tupiratins (−8.3917, −48.1114, WGS 84; Fig. 1A). This area was chosen because it has five dams upstream so that cumulative impacts of dams could be studied. Also, continuous flow data collected by the Agência Nacional das Águas (ANA) during the study period was available for this section of the river but not others. The section of river has a floodplain of approximately 750 km^2 as delineated by the GFPLAIN250m floodplain boundary product (Nardi et al., 2019), which is based on the Shuttle Radar Topography Mission (SRTM) digital elevation model (DEM). In this dataset, STRM pixels with elevations lower than corresponding maximum channel flow level for the river were considered part of the floodplain. This stretch is located in the state of Tocantins in central eastern Brazil and is part of the Legal Amazon (Fig. 1A). The Tocantins River flows from south to north with its headwaters in the state of Goiás and drains into the Atlantic Ocean near the city of Belém in the state of Pará. The Tocantins River has a total drainage area of 767,000 km^2 with a mean annual discharge of approximately 11,000 $m^3\ s^{-1}$ (Fig. 1B, C; Costa et al., 2003). Suspended sediment concentration in this span of the Tocantins River ranges between 125 and 157 mg/L (Lima et al., 2003).

The Tocantins is the most dammed river in the Amazon, with six mega-dams (>15 m in height and generating over 400 MW of power) along with a smaller dam that generates more than 200 MW of power installed and two more mega-dams planned for construction (Akama, 2017; Table 1). The study site is downstream of five of the seven existing dams (Fig. 1A). The furthest upstream dam (Serra da Mesa) has a

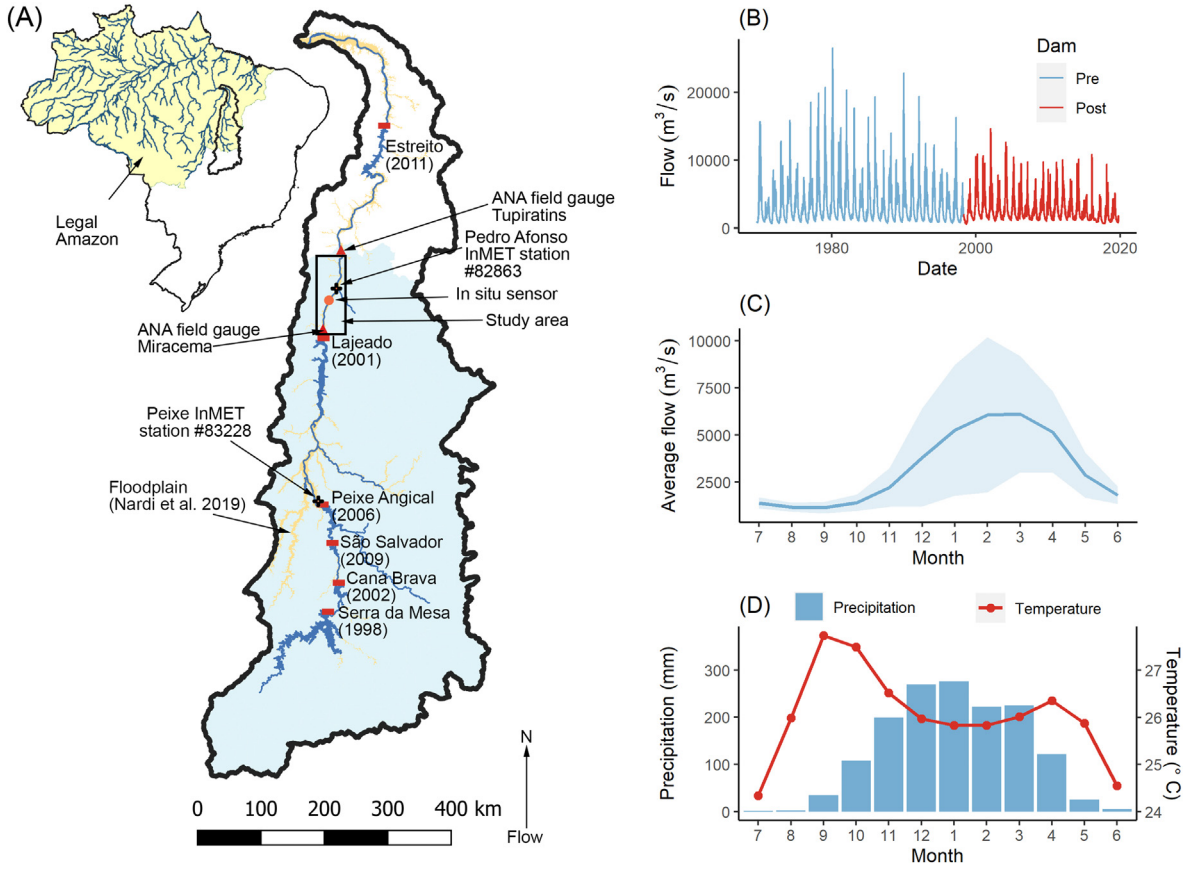

Fig. 1. (A) Tocantins River watershed from the headwaters to the confluence with the Araguaia River. Dams with opening years in parentheses are labeled. The rectangular area represents the study site. The light blue shaded area is the upstream contributing area for the Tupiratins ANA gauge, which defines the downstream boundary of the study area. (B) Daily and (C) average monthly flow measured at the Tupiratins gauge from 1969 to 2019. Blue shaded region is monthly flow range. (D) Mean monthly precipitation (blue bars) and temperature (red line) measured at the Peixe InMET station (Instituto Meteorologico; #83228) from 1975 to 2017. (For interpretation of the references to color in this figure legend, the reader is referred to the web version of this article.)

storage potential of 54.4 km^3. The other four dams upstream of the study area (Cana Brava, São Salvador, Peixe Angical, Lajeado) are all considered run-of-river dams and have smaller reservoirs, the largest of which (Lajeado, also known as Luis Eduardo Magalhães dam) has a maximum storage capacity of 5.2 km^3 (Table 1).

The Tocantins River runs through the Cerrado biome, a tropical savanna ecosystem with native vegetation comprised of open grassland to nearly closed canopy forest ranging from 12 to 15 m in height (Ratter et al., 1997). The tree layer in the Cerrado (savanna) may vary in density but occurs over a continuous shrub-herbaceous layer (Souza et al., 2020). The drought-tolerant Cerrado vegetation transitions into riparian forests (*matas ciliares*, Ribeiro and Walter, 1998), gallery forest surrounding small streams, and alluvial forests that occur on islands within the river channel (Ratter et al., 1997; Oliveira-Filho and Ratter, 2002). Approximately 13% of the Tocantins watershed lies within protected areas, the smallest proportion of any of the major watersheds within the Amazon (Trancoso et al., 2009). The watershed has undergone extensive land cover change due to conversion of savanna and forest to pasture and soy monoculture (Costa et al., 2003; Swanson and Bohlman, 2021).

The region has highly seasonal precipitation (yearly mean = 1500 mm, monthly range = 1–296 mm; Fig. 1D). October through March is the wet season (≈140–250 mm/month rainfall), and April through September is the dry season (<10 mm/month rainfall; Costa et al., 2003; Klink and Machado, 2005). This seasonality in precipitation leads to a regular seasonal flooding pattern throughout the watershed. A previous study has shown no significant change in precipitation patterns in the Tocantins River basin since the 1970s (Coe et al., 2008).

3. Materials and methods

To quantify dam-induced changes to floodplain extent, hydroperiod, and inundation timing across the study region, we created daily floodplain inundation maps for the area. We then compared the flooding regime before and after each dam's operation, as well as comparing between the period before any dams were installed and after all five

Table 1
Large dams on the Tocantins River, listed in order of opening date. Dams listed in bold text are upstream of the study area and were included in the analysis.

Dam name (abbr)	Opening date	Type	Reservoir volume (km^3)	Energy capacity (MW)
Tucuruí	December 30, 1984	Storage	45.0	8370
Serra da Mesa (SDM)	April 30, 1998	Storage	54.4	1275
Lajeado (LJCB)	December 1, 2001	Run-of-river	5.2	902.5
Cana Brava (LJCB)	May 22, 2002	Run-of-river	0.5	450
Peixe Angical (PEAN)	June 7, 2006	Run-of-river	2.7	500
São Salvador (SASA)	August 6, 2009	Run-of-river	1.0	243.2
Estreito	April 29, 2011	Run-of-river	1.4	1087

were operational. The pre-dam period in this study spans from 1985 to 1997 based on data availability. From 1998 onward, the river had at least one dam upstream with additional dams operational at various dates (Fig. 1A; Table 1). We considered the effects of each additional dam separately, except for the Lajeado and Cana Brava dams, which were considered together since they were opened within six months of each other. We refer to the time periods between individual dams based on the name of the dam installed at the beginning of the time period. During the last eleven years of the study period, from 2009 to 2019, all five upstream dams were operational, and no new dams were installed. We also independently measured floodplain water level for one year in the field to validate the flooding maps we created using the water level data.

3.1. Floodplain inundation estimation

Water level data came from two Agência Nacional das Águas (ANA) flow gauge stations located near Miracema do Tocantins (station ID #22500000) and Tupiratins (station ID #23100000; Fig. 1A). These two stations were selected from 117 candidate stations on the Tocantins River because they were adjacent to each other on the river and had the most complete data from 1985 to 2019. The Miracema do Tocantins station had 214 missing daily values over the 34-year period (<1.7%) while Tupiratins had 49 missing days (0.4%). Missing days were filled by developing and applying linear regressions using all available daily data between the Miracema and Tupiratins stations with three other nearby stations. Water level correlations between these stations ranged from 0.93 to 0.97.

Using daily data from the Miracema and Tupiratins stations, we then linearly interpolated water surface elevation across the ≈145-km river reach between the two stations using the seq function in R (R Core Team, 2020) and the Qchainage plugin in QGIS v. 3.4.1 to evenly space interpolated points every 2 km. As the Tocantins River has a very low slope (≈1 cm km^{-1}), the 2-km spacing would result in a water elevation error of approximately 2 cm, substantially less than the 1-m elevation resolution of the digital elevation model used for deriving terrain elevation across the study region.

To represent floodplain topography, we used the 2010 1 arc-second digital elevation model (DEM) from the Shuttle Radar Topography Mission (SRTM) clipped to the study region. Using the interpolated water level points as centroids, we created a series of rectangular boxes approximately 2 km in river length (upstream-downstream) and extending 20 km in width perpendicular to the river to capture the entire floodplain and adjacent uplands. We filled each 1 arc-second cell in the rectangular box with the water level value from its centroid. For cells that overlapped (e.g., around river bends), we used the average water level of the overlapping cells. To estimate water level in each cell, we subtracted the DEM topography value for each cell from the daily water elevation value for that cell. The cell was considered flooded on any day if the result was positive and not flooded if the result was zero or negative. We then mosaicked the buffers to create a continuous floodplain landscape over the entire study area. Data were aggregated at daily, seasonal, and yearly timesteps to investigate patterns in flood timing and duration and extent of flooded area before and after damming.

To examine the effects of each additional dam, we subdivided the study into five different time periods: before any dams (July 1, 1985–June 30, 1997), after Serra da Mesa dam (July 1, 1998–June 30, 2001), after Lajeado and Cana Brava dams (July 1, 2002–June 30, 2006), after Peixe Angical dam (July 1, 2006–June 30, 2009), and after São Salvador dam (July 1, 2009–June 30, 2019). We used water years (July 1–June 30) to examine changes in floodplain hydrology because the rainy season occurs from November through April in the study region and excluded leap days so we could compare across all years. We also excluded the 1998, 2002, and 2018 water years because dams became operational partway through 1998 and 2002 (Table 1) and because of anomalies in the water level data during 2018. For date of first inundation, we converted dates to numerical values (where July 1 = 1 and June 30 = 365).

We measured flooded extent (i.e., a measure of magnitude) as the maximum area flooded in any given water year, or in the wet (November–April) or dry (May–October) season. For hydroperiod (i.e., a measure duration) and first day of inundation (i.e., a measure of timing), we only considered pixels that were inundated for at least one day in every year across the entire study period, which we call the "core inundated area". Excluding pixels that were only inundated in some years allowed us to describe changes in duration and timing within the portion of the floodplain that still consistently flooded after damming. The core inundated area comprised 6.2 km^2, representing approximately 5% of the average pre-dam flooded area and 19% of the average post-dam flooded area. Hydroperiod was calculated as the total number of days each pixel was flooded during each water year, and first day of inundation was the first day each pixel was flooded during each water year. For timing, we measured the first day of flooding because this metric should be closely related to the onset of the rainy season when high flow events in the river begin and is likely to be related to riparian forest phenology.

To understand how flooded extent, hydroperiod, and first day of inundation changed as more dams were added, we modeled these responses as a function of number of dams (0–5) using generalized additive models (GAM), which account for non-linear relationships using smoothing splines. For flooded extent and hydroperiod, which were measured at annual or seasonal timesteps, we accounted for rainfall by including total annual (or wet/dry season) rainfall as a non-linear covariate. For first day of inundation, we added the day of year when cumulative precipitation reached 10% of its annual total (i.e., a measure of the onset of the wet season) as a non-linear covariate. Hydroperiod and first day of inundation were modeled for each pixel in the core inundation area. Because these pixels were likely spatially autocorrelated, which could lead to significance inflation, we accounted for spatial dependency by adding the xy-coordinate of each observation as a non-linear covariate. Flooded extent did not have spatial dependency because it was measured as a single value (maximum flooded area) for each year or season. All GAMs were fitted with a gamma log link function using the bam function from the mgcv package (Wood and Wood, 2015). Model formulas can be found in Appendix B, Figs. B1, B2, and B3.

To understand how damming affected the variance in flooded extent, hydroperiod, and flood timing, we also tested for pre- and post-dam differences in variance for all three hydrologic variables with a Brown-Forsythe test, which is more robust to violations of normality than a standard F test (Brown and Forsythe, 1974). For this analysis, we lumped all time periods with more than one dam as 'post-dam' because of the short windows between additional dam operations and used the bf.test function from the onewaytests package (Dag et al., 2018) in R.

3.2. Field validation

We compared our inundation maps to water level measured in the field using a pressure transducer installed in the floodplain. We placed a HOBO U20-001-02 water level logger (Onset Company, Cape Cod Massachusetts, USA) in the Tocantins River floodplain near the town of Pedro Afonso, approximately 50 km downstream of the Miracema do Tocantins station (Fig. 1A). The logger was hung from fishing line placed inside of a perforated polyvinyl carbonate (PVC) well fitted with a nylon mesh to minimize siltation. We buried the well 50 cm into the ground and left it stationary for the duration of the data collection period. The logger collected total pressure and temperature data in 15-minute intervals from August 9, 2018 to August 25, 2019. We downloaded data every three months using a HOBO Base-U-4 base station and then replaced the water logger into the well. We used HOBOware Pro v. 3 to convert pressure data (kPa) into water level (cm) based on the

software-provided relationships between pressure, temperature, and water level. Total pressure data were converted to water pressure using barometric pressure data collected by the Pedro Afonso InMET station (Instituto Nacional de Meteorologia; #82863) 23 km away from the HOBO sensor location (Fig. 1A).

To determine whether a flooding event occurred at our field point on any given day, we temporally aggregated the 15-minute water level data. Because information on how the ANA water level data was measured was not available, we considered three criteria (minimum, mean, and maximum recorded water level) to determine if the data logger location was flooded on a given day and compare it with floodplain inundation values derived from ANA and the SRTM DEM data at the same location. The values for inundation in both the field data and modeled floodplain inundation maps were binary (i.e., 1 for inundated, 0 for not inundated). We used a confusion matrix (flooded versus not flooded) to compare the accuracy of daily flooding events derived from our modeled floodplain inundation maps to the daily flooding events collected in the field.

The in-situ sensor and inundation maps have different temporal resolution and spatial coverage. The DEM (and inundation maps derived from it) only measure elevation in increments of 1 m, whereas the in-situ logger produced values in increments of 0.41 cm. Additionally, each 1 arc-second DEM pixel contains only one elevation value, so changes in elevation at smaller scales will be missed. To incorporate variation in land surface elevation that might be missed due to the pixel resolution, we performed a secondary analysis by smoothing the SRTM DEM using the average elevation of the neighboring eight pixels for the point where our field data logger was located. We subtracted the smoothed elevation value from the ANA water level to determine whether and how the DEM elevation value affected our modeled floodplain inundation maps when compared to the in-situ data.

3.3. Climate and land cover change analysis

To assess whether changes in floodplain inundation could have been driven by temporal variation in rainfall or land cover, we also assessed temporal trends in land cover-flow relationships and precipitation. We used the Climate Research Unit's CRU TS v. 4.03 gridded rainfall data (CRU; Harris et al., 2020), land cover data from MapBiomas v. 4.1 (Souza et al., 2020) and flow data collected by ANA at the Tupiratins station, which was the station furthest downstream of the stretch of river being studied. The Climate Research Unit Time Series (CRU TS) rainfall data is measured at a $0.5° \times 0.5°$ (approximately 50×50 km) spatial resolution, while MapBiomas has a 30×30 m resolution due to the resolution of the Landsat data from which it is derived. Both datasets have a yearly temporal resolution. Precipitation and land cover data were measured over the upstream contributing area of our most downstream measurement location (Fig. 1A) using the HydroBasins v. 1.0 level 8 demarcation (Lehner and Grill, 2013). The upstream contributing area includes the portion of the river from the headwaters to the Tupiratins station, along with all tributaries that flow into the river in that region. We calculated the mean annual precipitation from gridded monthly data over the upstream contributing area, then performed a Mann Kendall regression (Marengo et al., 1998) using the Kendall package in R (McLeod and McLeod, 2015) to assess whether there was a temporal trend in rainfall over the study period. We converted daily discharge ($m^3\ s^{-1}$) at the Tupiratins station to specific discharge ($m\ s^{-1}$) by dividing by the upstream contributing area and aggregated to yearly averages to match the temporal resolution of the precipitation and land cover data. We then divided specific discharge by annual precipitation to determine the proportion of precipitation realized as flow in each year and investigated how this quantity varied over time. Because the most common land use change in the area was from natural cover (e.g., forest, savanna) to pasture, we related precipitation-scaled specific discharge to the proportion of pasture cover in the upstream contributing area. We performed a simple linear regression to relate the two variables both over the entire study period (1985–2019) and separated by pre- and post-damming periods.

To determine whether changes in first day of inundation compared across damming periods were related to changes in onset of rainfall over the course of our study, we tested whether there was a significant change in the onset of the rainy season, measured as day of year when 10% of the annual rainfall had fallen. We performed an ANOVA to determine whether there was a significant difference in rainy season onset between the different damming periods. For this analysis, we used rainfall measured daily at the Peixe InMET station (#83228). The Peixe InMET station is located near the city of Peixe Angical (Fig. 1A) and was the only climate station in the upstream contributing area with a complete daily precipitation time series for the study period.

4. Results

4.1. Field validation

Modeled floodplain inundation maps predicted observed site inundation with an accuracy of 0.88 (95% confidence interval (CI): 0.84–0.91) when using mean daily data from the field sensor (Table A1). Using minimum daily water level increased accuracy to 0.93 (CI: 0.90–0.95), while aggregating by maximum daily water level had the lowest accuracy (0.83, CI: 0.79–0.87). Overall, modeled floodplain inundation maps consistently underpredicted flooding events (Table A1, Fig. 2). This may be because the vertical resolution of the DEM (1 m) and resulting modeled inundation map caused flooding events of less than a meter of water level to be missed. Additionally, ANA only reports one value for water level each day, which may not capture ephemeral flooding events lasting less than a single day that

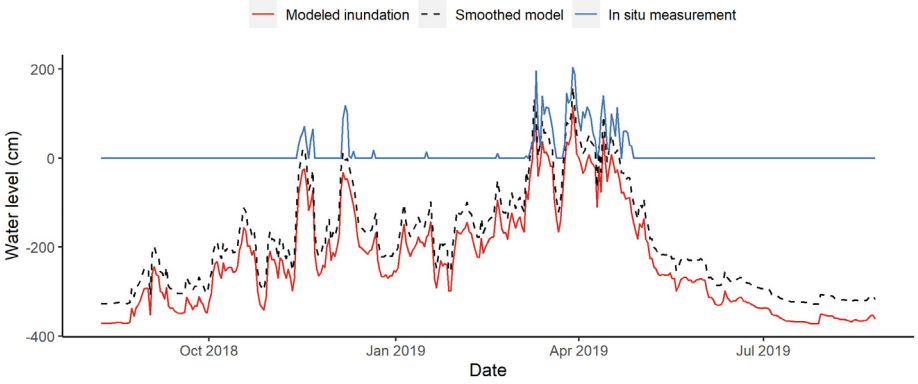

Fig. 2. Comparison of flood events captured by field collection (mean daily water level > 0; blue) and models based on water level and elevation near Pedro Afonso, Tocantins. Flat blue line for in-situ indicates water level is below surface. (For interpretation of the references to color in this figure legend, the reader is referred to the web version of this article.)

were captured by the in-situ sensor. However, the general pattern of inundation frequency and timing is similar between modeled data and data collected in-situ (Fig. 2), indicating that our floodplain models are capturing overall patterns of inundation but underestimating flooding by some scalar factor. Modeled floodplain map accuracy increased when we used the elevation value from the smoothed DEM and field data aggregated to daily means (0.94; CI: 0.91–0.96). For the smoothed DEM and field data aggregated by maximum and minimum daily inundation, accuracy was 0.90 (CI: 0.86–0.92) and 0.96 (CI: 0.93–0.98), respectively (Table A1).

4.2. Flooded extent

Average flooded extent decreased from 132.1 km^2 to 48.7 km^2 after the first dam, Serra da Mesa, was installed (Fig. 3A). During the Lajeado/Cana Brava period (2003–2006), mean flooded extent increased to 52.5 km^2 before decreasing to 37.0 km^2 after the installation of Peixe Angical and 31.8 km^2 after all dams were installed. Annual maximum flooded extent was significantly related to the number of dams on the river ($p < 0.001$) as well as the total annual rainfall ($p < 0.01$; Fig. B1A). There was also significantly lower variance in flooded extent pre-dam versus post-dam ($p < 0.05$; Table B1). Specifically, before any dams were installed, maximum annual flooded extent ranged from 30.7 km^2 to 438.9 km^2 (Fig. 4). After all dams were installed, this range was reduced to 8.0 km^2 to 70.0 km^2 (Fig. 4).

Changes in maximum flooded extent during the wet season closely follow annual patterns, decreasing from an average of 131.1 km^2 before any dams to 31.9 km^2 after all dams were installed on the river (Fig. 3B). Maximum wet season flooded extent was significantly related to the number of dams on the river ($p < 0.001$) and total wet season rainfall ($p < 0.05$; Fig. B1B). Variance in wet season flooded extent was significantly different between pre- and post-dam periods ($p < 0.05$; Table B2). Unlike the wet season, dry season flooded extent did not show a clear trend of decreasing through time (Fig. 3C). Dry season maximum flooded extent was significantly related to total dry season rainfall ($p < 0.05$) but not to number of dams ($p = 0.22$; Fig. B1C). There was also no significant difference in variance in between pre- and post-dam flooded extent during the dry season ($p = 0.21$; Table B3).

4.3. Hydroperiod

Hydroperiod of the core inundated area (pixels that were inundated at least one day per year during the whole study period) declined as more dams were added to the river, after accounting for total annual rainfall and spatial dependency between pixels ($p < 0.001$, Fig. B2). Mean hydroperiod decreased from 141 days pre-damming to 126 days after Serra da Mesa was installed (Fig. 5A). After all five dams were installed on the river, average hydroperiod decreased to 91 days (Fig. 5B). The mode of the distribution of per-pixel hydroperiod shifts from 122 days pre-damming to 12 after all dams installed (Fig. 5B). The variance in hydroperiod was also significantly lower between pre- and post-damming periods ($p < 0.001$; Table B4). In addition to declines in average hydroperiod for the core inundation area, it is important to reiterate that the vast majority of low-hydroperiod pixels no longer flooded after damming (Figs. 4 and D1).

4.4. Flood timing

For the core inundated area, the first day of inundation was significantly related to number of dams on the river after accounting for onset of rainfall, which was also significantly related to first day of inundation ($p < 0.001$; Fig. B3). Mean first day of inundation prior to damming was day 161 (December 8). After Serra da Mesa was installed, the mean first day of inundation was day 156 (December 3). However, once all dams were installed on the river, the mean first day of inundation was day 173 (December 20). Variance of first day of inundation was significantly higher pre-damming versus post-damming ($p < 0.001$; Table B5).

First day of inundation of the core inundated area was significantly related to the onset of the rainy season, as measured by the day of year when cumulative rainfall reached 10% of the annual total ($p < 0.001$). The date of rainy season onset did not vary significantly

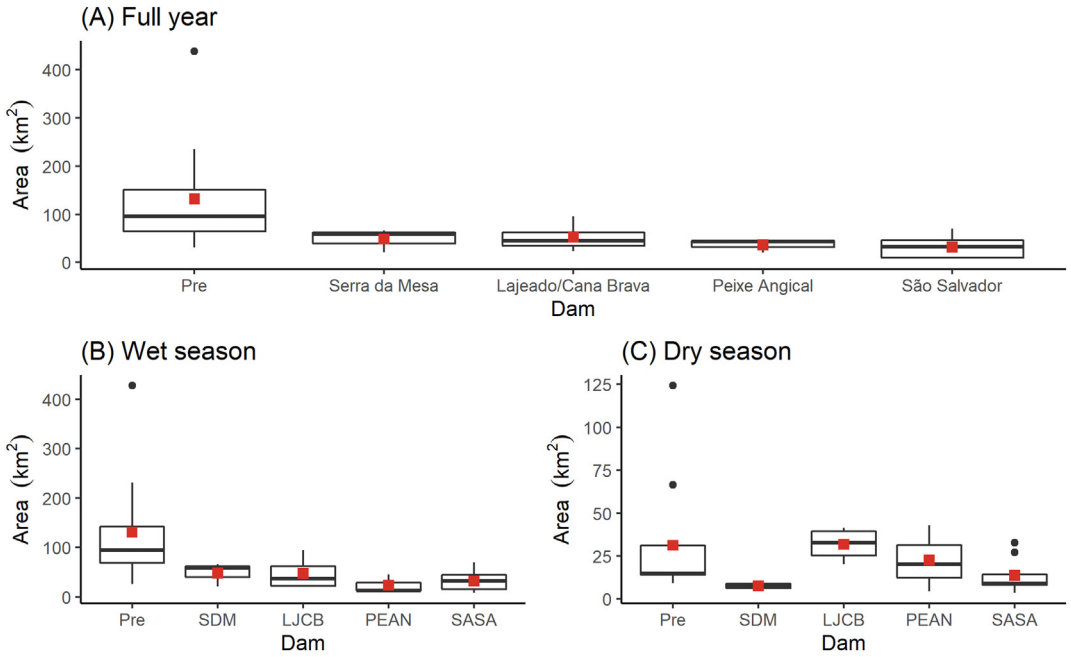

Fig. 3. Boxplots for maximum flooded extent for (A) the full year, (B) wet season, and (C) dry season. Line within the box represents the median, red dot is the mean, and the limits of the box are the interquartile range. SDM stands for Serra da Mesa, LJCB for Lajeado/Cana Brava, PEAN for Peixe Angical, and SASA for São Salvador. Dams are ordered by opening date. Note the y-axis for the dry season is smaller than those of the full year and wet season. (For interpretation of the references to color in this figure legend, the reader is referred to the web version of this article.)

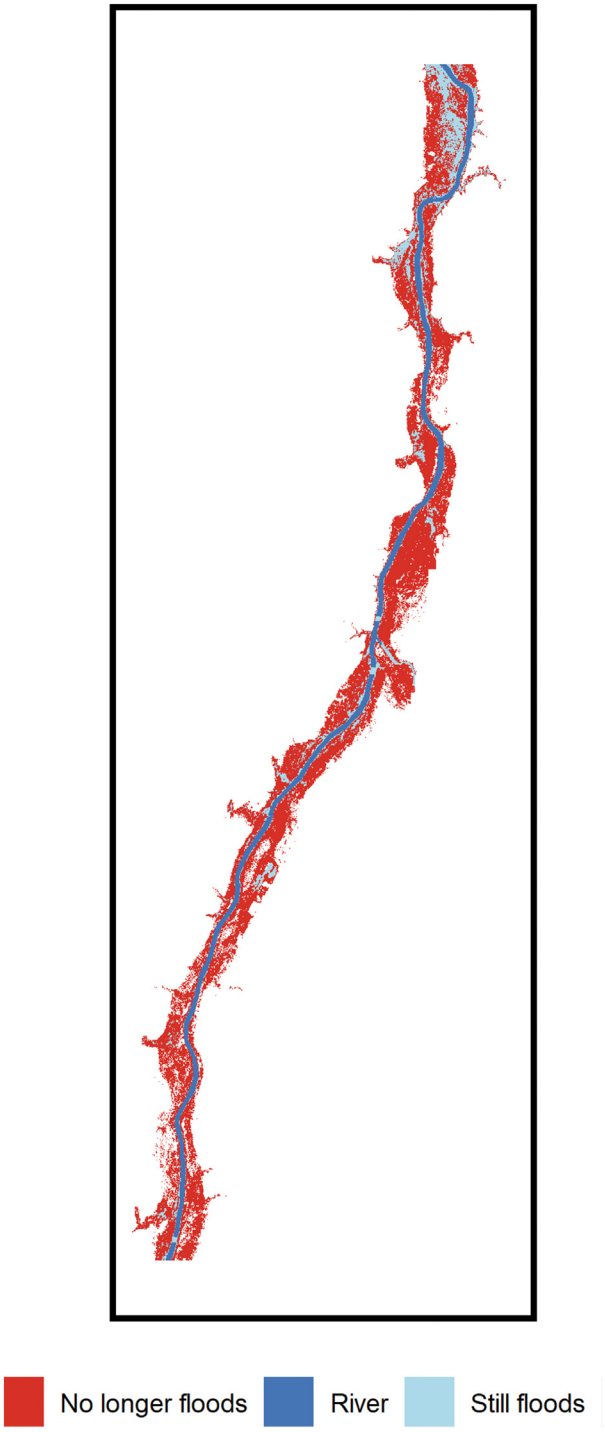

Fig. 4. Changes in maximum flooded extent after all five dams were installed on the Tocantins River. Red and light blue areas indicate the maximum flooded extent of the pre-dam floodplain. Light blue pixels indicate areas that still flood after the installation of all five dams (16% of pre-dam maximum flooded area). Fig. C1 shows the underlying topography of the study area. (For interpretation of the references to color in this figure legend, the reader is referred to the web version of this article.)

among damming periods ($p = 0.1$; Table E1), however we found that the lag time between the start of the rainy season and first day of inundation differed significantly between damming periods ($p < 0.001$; Table E2). Average lag time between first day of inundation and the onset of the rainy season was 39 days prior to damming but increased to 51 days after all five dams were operational (Figs. 6 and E1).

4.5. Cumulative impacts of dams

The Serra da Mesa dam, the first installed upstream of the study area, had the largest impact on floodplain hydrology. Our models suggest that the addition of more dams on the river continues to decrease hydroperiod of the core inundated area and flooded extent but at decreasing rates (Figs. B1, B2). For the core inundated area, the operation of additional dams on the river pushed flood timing later in the year, but only up to the installation of the fourth dam (Fig. B3). Collectively these results suggest that eventually, the system will reach a critical point where adding more dams does not further alter floodplain hydrology.

4.6. Climate and land cover change

There was no significant linear trend in mean annual precipitation over the study period ($p = 0.30$; Fig. 7A), however there was a strong and significant decrease in mean annual flow ($p < 0.001$; Fig. 7B). Pasture in the upstream contributing area (Fig. 1) increased from 19% to 30% over the study period (Fig. E2), during which time the river was also being dammed, making it difficult to disentangle the individual contributions of climate, damming, and land cover change on observed changes in floodplain inundation patterns. However, when we scaled mean annual specific discharge (i.e., mean annual flow divided by contributing area) by mean annual precipitation, we found a consistently negative relationship with percent pasture in the upstream contributing area, which is opposite of the expectation that specific discharge would increase as pasture increased (Fig. 8; Costa et al., 2003). The slope of this relationship was stronger (more negative) in the post-dam period (Fig. 8). In other words, the proportion of precipitation realized as flow consistently declined over the study period, even as the land cover was converted from native Cerrado vegetation to pasture, and this trend was stronger and significant after damming ($p < 0.05$). Because the trend of decreased proportion of precipitation realized as flow vs. land cover only became significant after damming, we believe that this is because of the dams' effect on flow, not because of conversion of natural cover to pasture, which occurred at a nearly linear rate during the entire study (Fig. E2). Altogether, these patterns point to river flow, and therefore water level and floodplain inundation, being more affected by damming than by climate or land cover change.

5. Discussion

Damming of the Tocantins River coincided with large changes in floodplain hydrology. As we predicted, damming of the river decreased flooded extent, although only in the wet season. Our hypothesis that the flooded extent would be larger in the dry season was unsupported. After damming, hydroperiod in the core inundated area was shorter and floods started later in the wet season, supporting our predictions. The addition of dams on the river further decreased flooded extent and hydroperiod and led to a later start in flooding. There was no trend in regional rainfall during the study period. Though there was extensive land cover change during the study period, the trend we measured between deforestation and river flow was opposite to what we expected (i.e., deforestation leading to increases in precipitation-scaled specific discharge). Taken together, these analyses point to damming greatly altering river flow and floodplain hydrology. As seen in other dammed systems, changes in floodplain hydrology of the Tocantins River are likely to impact biophysical and ecological systems and humans who live in riverine communities.

5.1. Biophysical, ecological, and social impacts

Disruptions in connectivity between the river and floodplain wetlands, such as those shown here for the Tocantins system, can lead to important geomorphological changes (Hupp et al., 2009). We found that 86% of the former Tocantins floodplain no longer floods after damming. These areas that no longer flood are likely to experience a drastic decrease in

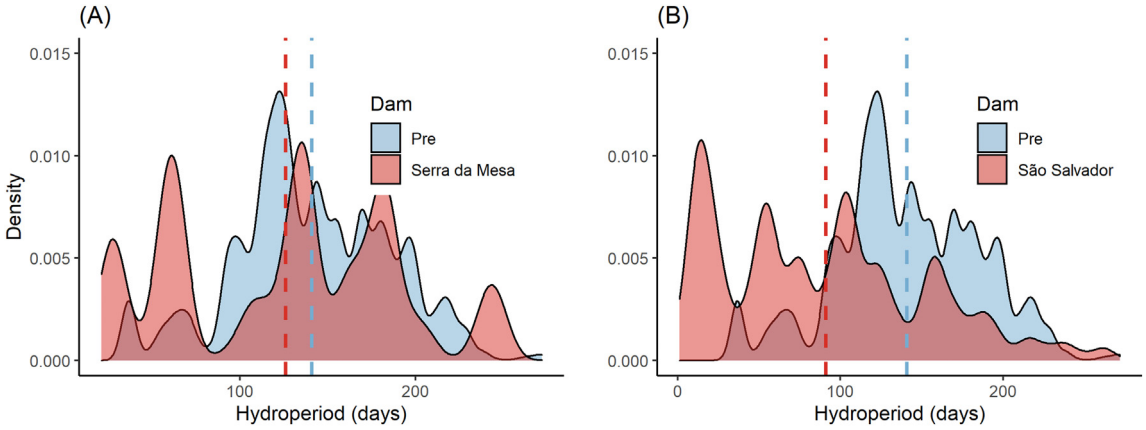

Fig. 5. Density plots of per-pixel hydroperiod for each pixel in the core inundated area for (A) all years before damming (1986–1997) and all years after the Serra da Mesa dam (1999–2001) and (B) all years before damming (1986–1997) and all years after all dams were operational (2010–2019). Blue dashed line represents mean hydroperiod before damming; red dashed line represents mean hydroperiod after damming. (For interpretation of the references to color in this figure legend, the reader is referred to the web version of this article.)

sediment deposition, whereas the small proportion of near-shore areas that still flood may have increased sediment deposition leading to the formation of levees that can further impede river-floodplain connectivity (Pearson et al., 2016; Li et al., 2017). Moreover, since floodplains transform and serve as major sinks for NO_3-N and other nutrients (Gergel et al., 2005), the reduction in river-floodplain connections shown here for the Tocantins basin has the potential to increase NO_3-N concentrations in the river. The Tocantins watershed is simultaneously undergoing land cover conversion from native savanna and forest ecosystems, which uptake nitrogen, to pasture and agricultural systems (Swanson and Bohlman, 2021) that often have added nitrogen loads that end up as runoff. Taken together, increased agricultural runoff coupled with decreased NO_3-N processing potential in the floodplain may to lead to downstream river and reservoir eutrophication, a widespread issue on dammed Brazilian rivers (Tundisi et al., 1993; Fontana et al., 2014).

The changes in river and floodplain hydrology quantified here will also impact the ecology of the Tocantins system via disruptions in longitudinal (upstream/downstream) and lateral (river-floodplain) connectivity, as well as changes in flood timing and hydroperiod. Specifically, the presence of five dams (and reservoirs) on this stretch of the Tocantins represents a major longitudinal disruption, which has been shown to reduce fish populations, especially of long-distance migrators, despite efforts to provide fish passage (Agostinho et al., 2007). Reproductive success of fish is also dependent on lateral connectivity, as the eggs of many species complete their development in the floodplain (Abrial et al., 2014). Changes in the flooded extent (86% reduction) and hydroperiod (35% shorter in the areas that still flood) of the Tocantins River floodplain are thus likely to reduce fish recruitment and reproductive success, lowering overall fish biomass within the river (Castello et al., 2015, 2019; Lima et al., 2016). Moreover, the delayed onset of flooding in the post-dam period (~2 weeks), combined with shorter-duration floods (i.e., the reduced hydroperiod found here) may lead to shorter spawning seasons and have the potential to alter fish community composition, favoring species that do not utilize the floodplain for feeding and reproduction (Agostinho et al., 2001; Abrial et al., 2014).

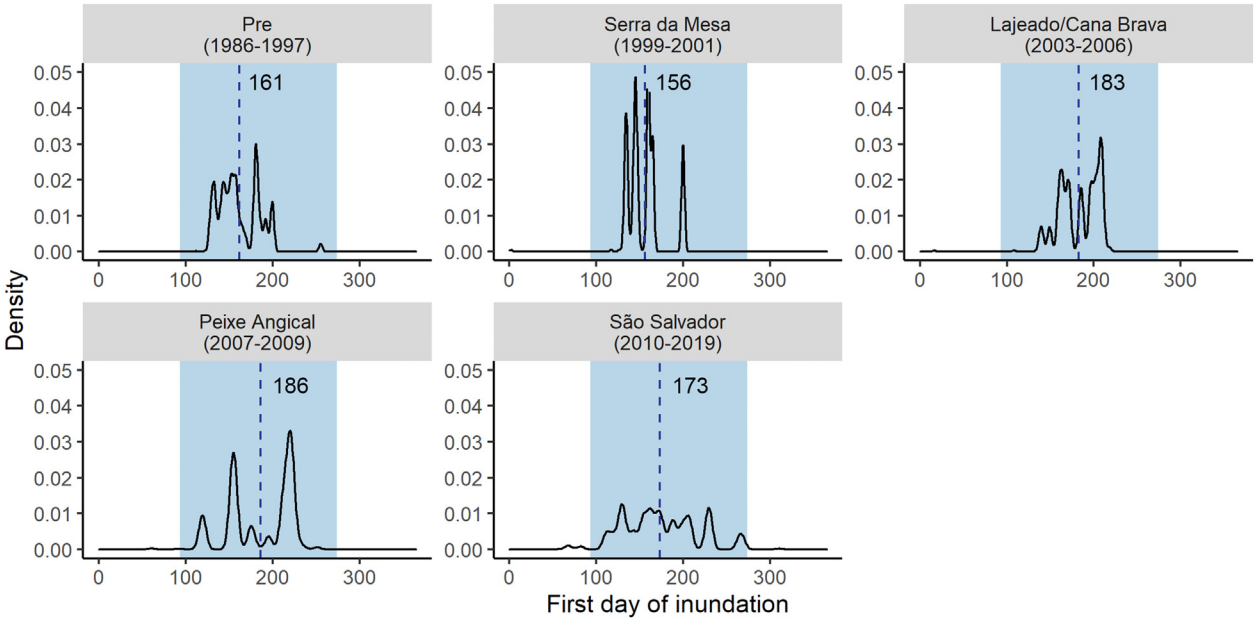

Fig. 6. Density plots for first day of inundation for the core inundation area separated by damming period. Density represents the proportion of pixels that were first inundated on a certain day of year. Blue shaded area corresponds to the rainy season (October–March). Dashed line and corresponding number represent the mean first day of floodplain inundation. (For interpretation of the references to color in this figure legend, the reader is referred to the web version of this article.)

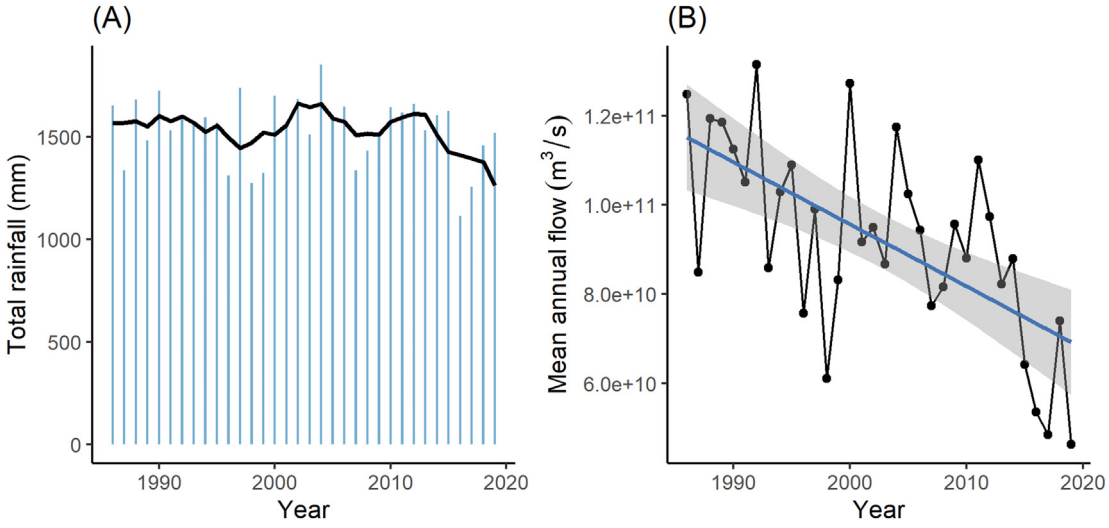

Fig. 7. (A) Total annual rainfall in the upstream contributing area collected by the Climate Research Unit from 1986 to 2019. Black line represents a 5-year rolling average of rainfall. Mann-Kendall regression showed no significant trend in rainfall over the study period. (B) Mean annual flow at the Tupiratins ANA station (#23100000) from 1986 to 2018. Blue line represents linear trend in mean annual flow over time. Shaded area represents the confidence interval of the linear trend. (For interpretation of the references to color in this figure legend, the reader is referred to the web version of this article.)

Phenological cues for many floodplain plants are also linked to flood timing and duration (Parolin and Wittmann, 2010; Parolin, 2012). Beyond the extirpation of floodplain plant species in areas that no longer flood, delayed flood timing may disrupt reproduction for species that reach peak fruiting during high flooding and have seeds dispersed by water (hydrochory) or fish (ichthyochory) (Kubitzki and Ziburski, 1994; Moegenburg, 2006; Horn et al., 2011). Coupled with disrupted hydrological cues for fish to spawn and move into the floodplain, plant species that disperse seeds through ichthyochory are likely to suffer severely reduced recruitment as a result of altered floodplain hydrology, leading to widespread changes in species composition (da Rocha et al., 2019). Overall, the hydrologic alterations observed here are likely to lead to considerable demographic and compositional changes in floodplain vegetative communities, with a trajectory toward species adapted to drier conditions (Nilsson and Dynesius, 1994) and causing riparian forests to transition to upland forests (de Lobo et al., 2019; Latrubesse et al., 2020).

Ecological changes brought about by hydrologic alterations in the floodplain have direct impacts on social and economic systems and are likely to negatively impact food security for river-dependent communities (World Commission on Dams, 2000). For example, downstream of the Tucuruí dam, installed on the Tocantins River in 1984, fish catch fell by 60% and shrimp harvests declined by 66%, leading to a decline in fishers in that region (Fearnside, 1999). Similar declines in fish catch have been reported in other dammed Amazonian rivers (Leite Lima et al., 2020). The loss of commercially important fish, which are often long-distance migratory species, can lead to overfishing as fishers switch to less commercially valuable species, a pattern seen across the Amazon (Doria et al., 2020). Beyond fisheries, many river-dependent communities on the Tocantins practice subsistence floodplain agriculture to supplement their diets (Laufer et al., 2020). Reductions in soil fertility from lack of regular flooding is thus likely to increase the cost of food production due to the need to purchase fertilizer (Laufer et al., 2020).

5.2. Cumulative impacts of dams

Understanding cumulative impacts of dams is important for mitigating social-ecological impacts of cascading systems (Arantes et al., 2019; Athayde et al., 2019a). Cumulative impacts may be metric-dependent (Timpe and Kaplan, 2017), such as we found in our study where flooded

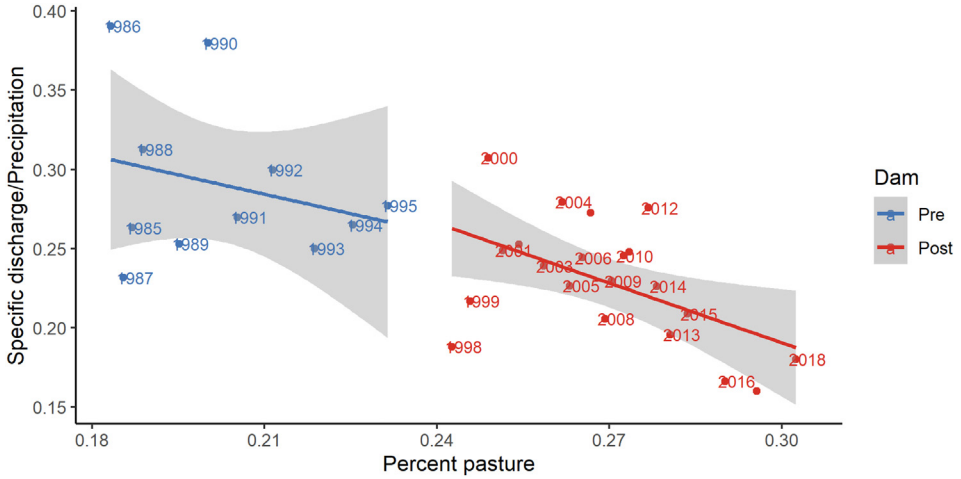

Fig. 8. Relationships between specific discharge divided by precipitation to percent pasture in the upstream contributing area. Blue points and line represent the pre-damming period while red points and line represent post-damming period. Shaded areas represent confidence intervals of the linear models. Numbers next to points are the year of each measurement. (For interpretation of the references to color in this figure legend, the reader is referred to the web version of this article.)

extent and hydroperiod were similarly affected by the addition of dams on the river while flood timing was not. Measuring impacts of additional dams on a river is challenging due to short time periods between dam installations and complex interactions between other environmental variables, such as seen in this system. In addition to changing hydrologic regimes in rivers and associated floodplains, cascading dams can also have ecological effects, such as decreasing fish abundance (dos Santos et al., 2018). Substantial knowledge gaps in understanding effects of cascade dams still exist, even as research into social-ecological impacts of dams has increased (Athayde et al., 2019b).

5.3. Climate and land cover change

Mean annual river flow showed a decreasing trend over the study period, however there was no significant trend in rainfall, indicating that the trend was not primarily driven by climate. We also found a significant negative relationship between precipitation-scaled specific discharge and percent pasture, but land cover change in the region is temporally correlated with damming. The conversion of forest to agriculture has previously been shown to *increase* river flow both in the lower reaches of the Tocantins (Costa et al., 2003) and downstream of its confluence with the Araguaia River (Coe et al., 2009). However, we saw the opposite trend, where conversion to pasture coincided with a decrease in flow (controlled for precipitation). Notably, Costa et al. (2003) measured flow before any of the dams were operational on the Tocantins River, while Coe et al. (2009) modeled only atmospheric, climactic, land cover, and flow variables, not accounting for extensive damming. Our finding that flow of the Tocantins River upstream of the confluence with the Araguaia is decreasing despite conversion from natural vegetation to pasture provides evidence that river damming is likely responsible for reducing mean annual flow in the Tocantins (and causing observed changes in floodplain hydropattern). Future analyses of relationships between land cover and flow in the Tocantins and other dammed rivers should also include impacts of damming in addition to climate and land cover variables.

5.4. Methodological considerations

Based on the comparison of flooding calculated from our inundation model versus the field sensor, the models may not capture short-duration flooding events and may thus underestimate flooded area and hydroperiod. However, since the model captured the temporal pattern in observed flooding well, including showing the pixel to be flooded during the wet season (Fig. 2), errors in our estimates of flooded extent are likely limited to pixels that flood only very briefly. Moreover, since any underestimates of flooded extent and hydroperiod would be consistent across the study period (including the pre- and post-dam periods), we are confident that the changes in these metrics we report are well represented by our model.

The location of this study was limited to a 145-km stretch of the Tocantins River because of lack of continuous data in other parts of the river, highlighting the importance of long-term, systematic data collection for future studies on impacts of infrastructure on social-ecological systems (Hyde et al., in review). Collecting continuous flow and water level data throughout the watershed would have enabled us to expand our study spatially, exploring areas downstream of fewer dams to further elucidate cumulative impacts of dams. The SRTM dataset is a high quality, openly available topographic model with higher vertical accuracy than other products, such as Advanced Spaceborne Thermal Emission and Reflection Radiometer (ASTER) and Global Multi-resolution Terrain Elevation Data (GMTED) (Thomas et al., 2014). However, SRTM-derived topography can still have errors in vertical resolution ranging from 8 m to over 16 m (Jarvis et al., 2004). These errors could lead to overestimation of inundation in areas where the topography is higher than that modeled by SRTM and underestimation of inundation in areas where the opposite is true. Improvements to this study could be made through use of a more refined DEM with sub-meter accuracy. With the advent of lidar technology in multiple formats, including a space-based sensor (Dubayah et al., 2020), such DEMs could be acquired for targeted regions at low expense. Finally, our methodology is limited to relatively narrow-channel rivers, as the geomorphology of braided and anastomosing rivers makes it challenging to accurately map floodplain inundation geometrically. For these rivers, remote sensing approaches including use of SAR (synthetic aperture radar) and optical remote sensing to detect flooding are likely to be more appropriate (Park and Latrubesse, 2017).

6. Conclusions and future directions

Our study provides insight into hydrologic changes in the floodplain of a highly dammed river. After damming, floodplain extent and hydroperiod both decreased and inundation started later in the year. This is one of only a few studies globally that investigates the cumulative impacts of multiple dams on a single river (e.g., Wang et al., 2017; Zhang et al., 2019). We show that cascade dams have cumulative, non-linear impacts, and these cumulative impacts are different dependent on the hydrologic metric, with flood extent and hydroperiod being most disrupted by the first dam and additional dams having a reduced effect on these two metrics. Understanding the impacts of damming across a floodplain landscape is important, given few rivers worldwide are still free-flowing. This study has implications for biophysical and ecological processes as well as for well-being and livelihoods of river-dependent peoples. Future studies could build on this research by expanding the geographic scale and measuring damming impacts from headwaters to mouth, which would allow researchers to further disentangle cumulative impacts of multiple dams by comparing impacts in areas with fewer dams to impacts in areas with more dams. Additionally, understanding the combined effects of damming and other anthropogenic impacts, such as deforestation, mining, and climate change, will be integral to modeling basin-wide hydrologic alteration and more accurately assessing environmental impacts of new dams (Castello and Macedo, 2016; Athayde et al., 2019a). As the Amazon basin is under increasing pressure from damming (Latrubesse et al., 2017; Anderson et al., 2018), understanding the impacts that dams have on this highly bio- and culturally diverse region is necessary to minimize and mitigate these impacts and preserve at least some segments of free-flowing river.

CRediT authorship contribution statement

A. Christine Swanson: Conceptualization, Methodology, Software, Validation, Formal analysis, Investigation, Resources, Data curation, Writing – original draft, Writing – review & editing, Visualization, Project administration, Funding acquisition. **David Kaplan:** Conceptualization, Methodology, Resources, Writing – review & editing, Supervision, Funding acquisition. **Kok-Ben Toh:** Methodology, Software, Formal analysis, Writing – review & editing. **Elineide E. Marques:** Resources, Writing – review & editing, Supervision, Funding acquisition. **Stephanie A. Bohlman:** Conceptualization, Methodology, Resources, Writing – review & editing, Supervision, Project administration, Funding acquisition.

Declaration of competing interest

The authors declare that they have no known competing financial interests or personal relationships that could have appeared to influence the work reported in this paper.

Acknowledgments

This research is partially based upon work supported by the National Science Foundation (NSF) [grant number 1617413]. Any opinions, findings, and conclusions or recommendations expressed in this article are those of the authors and do not necessarily reflect NSF views. ACS was supported by the University of Florida Water Institute; the University of

Florida Informatic Institute; and the Future Investigators in NASA Earth and Space Science and Technology program [grant number 80NSSC19K1255].

We would like to thank the 2015 University of Florida Water Institute Graduate Fellows Program, members of the Amazon Dams International Research network, and John Melack for early feedback on this study. Additionally, we thank Crysthiano Borges Pereira who assisted with field data collection in Brazil. Programa de Pós-Graduação em Ciências do Ambiente (PPGCiamb), Universidade Federal do Tocantins provided support for this project in Brazil. We would also like to thank Jasmeet Judge and Amr Abd-Elrahman for their input on this manuscript.

Appendix A. Confusion matrix for in-situ vs. modeled flooding events

Table A1
Confusion matrix results comparing modeled inundation maps to in situ data.

		Original elevation value		Smoothed elevation value	
		Inundation maps			
		Not inundated	Inundated	Not inundated	Inundated
Mean					
In situ data	Not inundated	321	0	321	0
	Inundated	46	15	22	39
Minimum					
In situ data	Not inundated	328	1	332	7
	Inundated	27	14	9	32
Maximum					
In situ data	Not inundated	303	0	303	0
	Inundated	64	15	40	39

Appendix B. Statistical results for floodplain hydrology

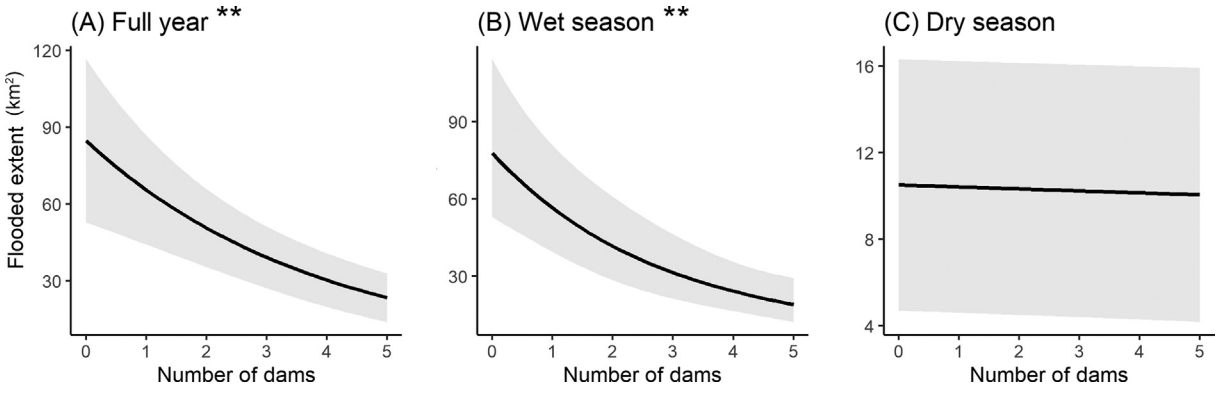

Fig. B1. GAM predictions for changes in flooded extent related to number of dams in (A) a full year (extent ~ number of dams + total annual rainfall); adjusted $R^2 = 0.43$, (B) the wet season (extent ~ number of dams + total wet season rainfall); adjusted $R^2 = 0.50$, and (C) the dry season (extent ~ number of dams + total dry season rainfall); adjusted $R^2 = 0.12$. Asterisks denote significant relationship ($p < 0.01$). To create these figures, we held rainfall constant at the mean total (A) annual, (B) wet season, and (C) dry season value (mm) for the entire study period. Shaded area is 95% confidence interval.

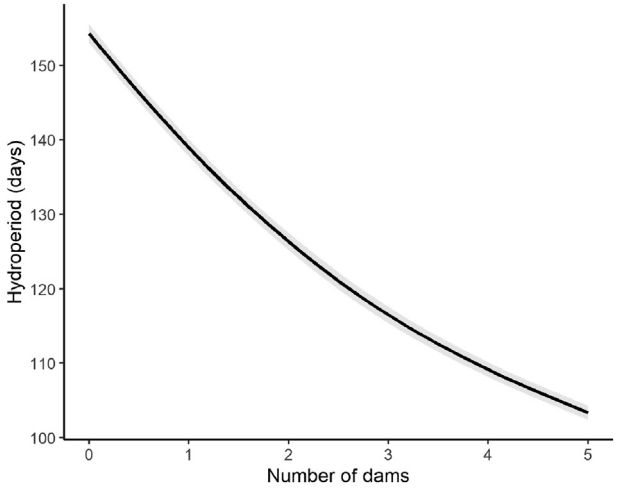

Fig. B2. GAM predictions for changes in hydroperiod of the core inundated area related to number of dams for a random pixel and mean total annual rainfall (mm) for the study period (hydroperiod ~ number of dams + total annual rainfall + xy). Shaded area is 95% confidence interval. Adjusted $R^2 = 0.37$. Figure was created holding annual rain constant at mean total annual rainfall for the entire study period for a location in the center of the study region.

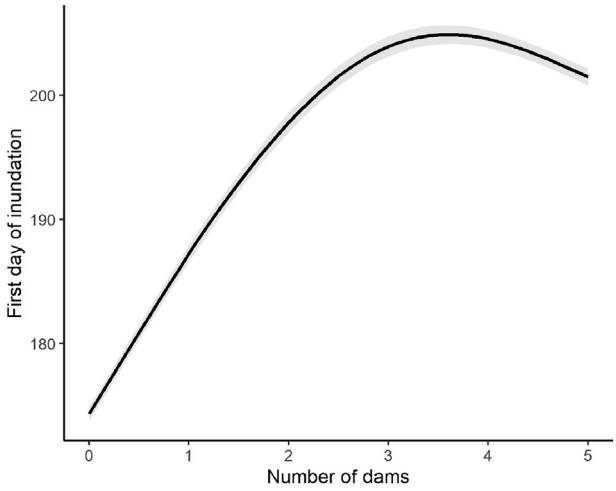

Fig. B3. GAM predictions for changes in first day of inundation of the core inundated area related to number of dams (first day of inundation ~ number of dams + onset of rainfall + xy). Shaded area is 95% confidence interval. Adjusted $R^2 = 0.39$. Figure was created holding day of year when precipitation reached 10% of total annual precipitation constant at the mean value across all years in the study at one x,y location in the study area.

Table B1
Results from Brown-Forsythe test for annual flooded extent (area ~ pre/post).

	Statistic	Degrees of freedom	*p* value
Pre/post	7.23	1	0.02

Table B2
Results from Brown-Forsythe test for wet season flooded extent (area ~ pre/post).

	Statistic	Degrees of freedom	p value
Pre/post	8.04	1	0.02

Table B3
Results from Brown-Forsythe test for dry season flooded extent (area ~ pre/post).

	Statistic	Degrees of freedom	p value
Pre/post	1.73	1	0.21

Table B4
Results from Brown-Forsythe test for hydroperiod (hydroperiod ~ pre/post).

	Statistic	Degrees of freedom	p value
Pre/post	30,078.41	1	<0.001

Table B5
Results from Brown-Forsythe test for first day of inundation (first inundation ~ pre/post).

	Statistic	Degrees of freedom	p value
Pre/post	9309.9	1	<0.001

Appendix C. Floodplain topography

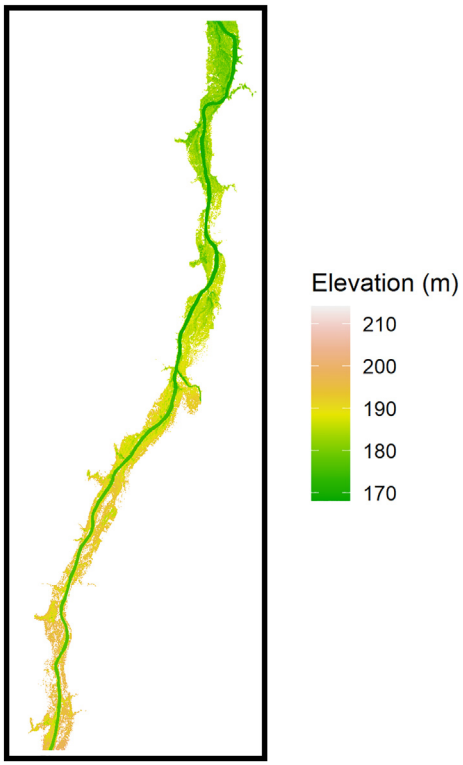

Fig. C1. Topographic map of the study area.

Appendix D. Hydroperiod histograms

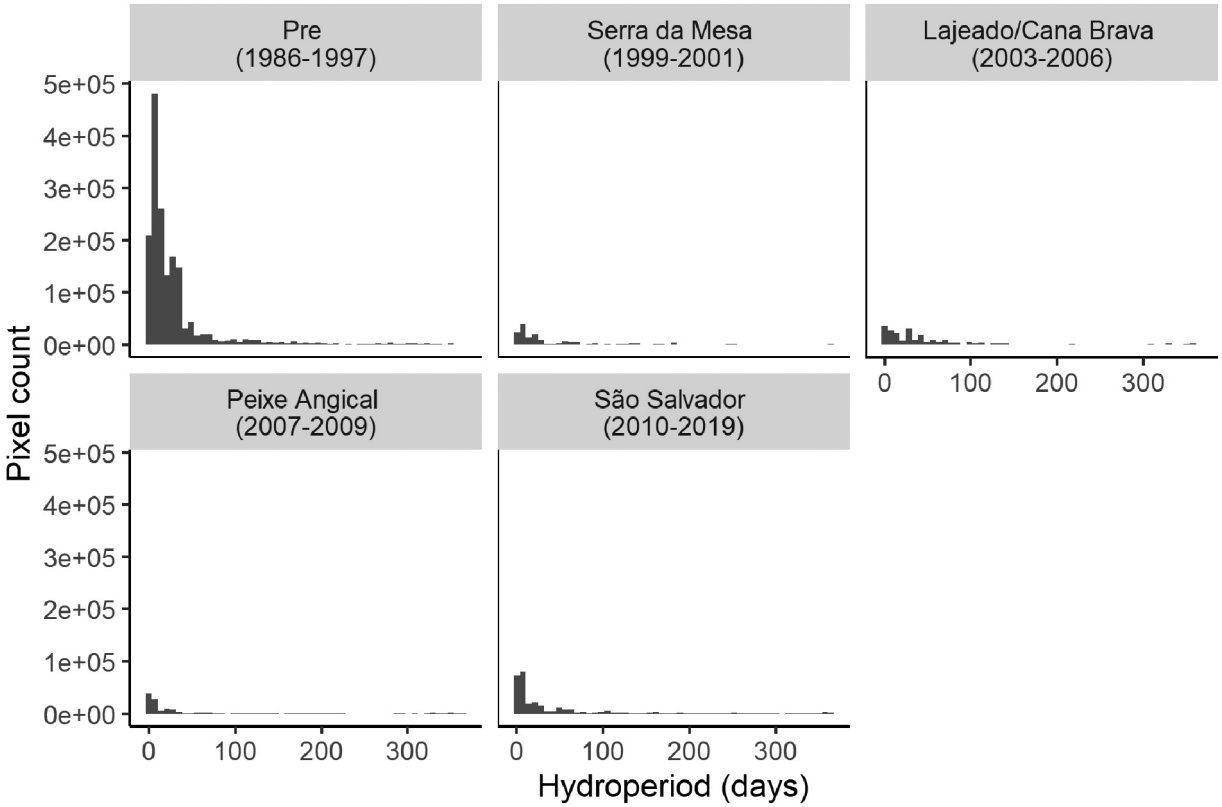

Fig. D1. Hydroperiod histograms for all pixels in the floodplain during each damming period.

Appendix E. Rainfall and land cover data and statistics

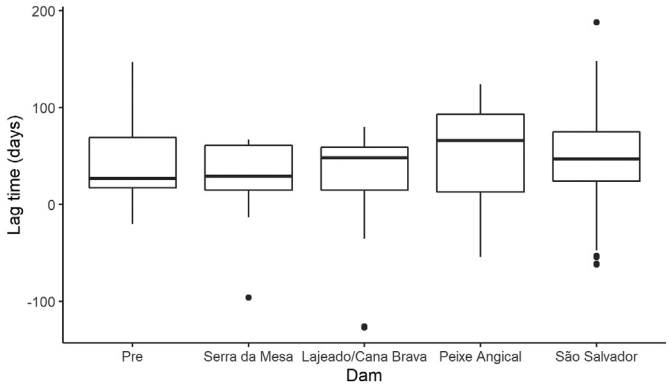

Fig. E1. Lag time between day of year when cumulative rainfall reached 10% of total annual rainfall and first day of inundation for all pixels in the core inundated area.

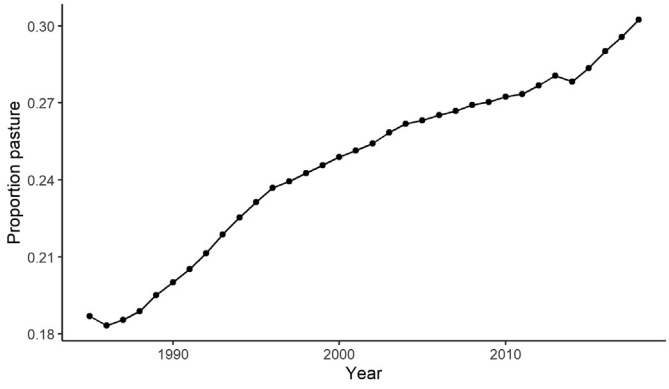

Fig. E2. Change in proportion pasture cover in the upstream contributing area over the study period.

Table E1
ANOVA results for onset of rainfall measured at the Peixe InMET station vs. dam period.

	Degrees of freedom	Sum of squares	Mean squared	F value	p value
Dam period	4	1735.1	433.8	2.2	0.10
Residuals	26	5094.6	196.0		

Table E2
ANOVA results for lag time between onset of rainfall and day of first inundation for each pixel for the core inundated area vs. dam period.

	Degrees of freedom	Sum of squares	Mean squared	F value	p value
Dam period	4	11,391,124	2,847,781	2629	<0.001
Residuals	196,915	213,304,058	1083		

References

Abrial, E., Rabuffetti, A.P., Espínola, L.A., Amsler, M.L., Blettler, M.C.M., Paira, A.R., 2014. Influence of hydrological changes on the fish community in two lotic environments of the middle Paraná floodplain, Argentina. Aquat. Ecol. 48, 337–349. https://doi.org/10.1007/s10452-014-9488-x.

Agostinho, A.A., Gomes, L.C., Zalewski, M., 2001. The importance of floodplains for the dynamics of fish communities of the upper river Paraná. Ecohydrol. Hydrobiol. 1, 209–217.

Agostinho, A.A., Marques, E.E., Agostinho, C.S., De Almeida, D.A., De Oliveira, R.J., De Melo, J.R.B., 2007. Fish ladder of Lajeado dam: migrations on one-way routes? Neotrop. Ichthyol. 5, 121–130. https://doi.org/10.1590/s1679-62252007000200005.

Akama, A., 2017. Impacts of the hydroelectric power generation over the fish fauna of the Tocantins River, Brazil: Marabá dam, the final blow. Oecologia Australis 21, 222–231. https://doi.org/10.4257/oeco.2017.2103.01.

Anderson, E.P., Jenkins, C.N., Heilpern, S., Maldonado-Ocampo, J.A., Carvajal-Vallejos, F.M., Encalada, A.C., 2018. Fragmentation of Andes-to-Amazon connectivity by hydropower dams. Sci. Adv. 4, eaao1642. https://doi.org/10.1126/sciadv.aao1642.

Arantes, C.C., Fitzgerald, D.B., Hoeinghaus, D.J., Winemiller, K.O., 2019. Impacts of hydroelectric dams on fishes and fisheries in tropical rivers through the lens of functional traits. Curr. Opin. Environ. Sustain. 37, 28–40. https://doi.org/10.1016/j.cosust.2019.04.009.

Arantes, C.C., Winemiller, K.O., Petrere, M., Castello, L., Hess, L.L., Freitas, C.E.C., 2018. Relationships between forest cover and fish diversity in the Amazon River floodplain. J. Appl. Ecol. 55, 386–395. https://doi.org/10.1111/1365-2664.12967.

Arias, M.E., Piman, T., Lauri, H., Cochrane, T.A., Kummu, M., 2014. Dams on Mekong tributaries as significant contributors of hydrological alterations to the Tonle Sap floodplain in Cambodia. Hydrol. Earth Syst. Sci. 18, 5303–5315. https://doi.org/10.5194/hess-18-5303-2014.

Assahira, C., Piedade, M.T.F., Trumbore, S.E., Wittmann, F., Cintra, B.B.L., Batista, E.S., et al., 2017. Tree mortality of a flood-adapted species in response of hydrographic changes caused by an amazonian river dam. For. Ecol. Manag. 396, 113–123. https://doi.org/10.1016/j.foreco.2017.04.016.

Athayde, S., Duarte, C.G., Gallardo, A.L.C.F., Moretto, E.M., Sangoi, L.A., Dibo, A.P.A., et al., 2019a. Improving policies and instruments to address cumulative impacts of small hydropower in the Amazon. Energy Policy 132, 265–271. https://doi.org/10.1016/j.enpol.2019.05.003.

Athayde, S., Mathews, M., Bohlman, S., Brasil, W., Doria, C.R., Dutka-Gianelli, J., et al., 2019b. Mapping research on hydropower and sustainability in the brazilian Amazon: advances, gaps in knowledge and future directions. Curr. Opin. Environ. Sustain. 37, 50–69. https://doi.org/10.1016/j.cosust.2019.06.004.

Bejarano, M.D., Sarneel, J., Su, X., Sordo-Ward, Á., 2020. Shifts in riparian plant life forms following flow regulation. Forests 11, 518. https://doi.org/10.3390/F11050518.

Brown, M.B., Forsythe, A.B., 1974. Robust tests for the equality of variances. J. Am. Stat. Assoc. 69, 364–367. https://doi.org/10.1080/01621459.1974.10482955.

Castello, L., Bayley, P.B., Fabré, N.N., Batista, V.S., 2019. Flooding effects on abundance of an exploited, long-lived fish population in river-floodplains of the Amazon. Rev. Fish Biol. Fish. 29, 487–500. https://doi.org/10.1007/s11160-019-09559-x.

Castello, L., Isaac, V.J., Thapa, R., 2015. Flood pulse effects on multispecies fishery yields in the lower Amazon. R. Soc. Open Sci. 2. https://doi.org/10.1098/rsos.150299.

Castello, L., Macedo, M.N., 2016. Large-scale degradation of amazonian freshwater ecosystems. Glob. Chang. Biol. 22, 990–1007. https://doi.org/10.1111/GCB.13173.

Coe, M.T., Costa, M.H., Howard, E.A., 2008. Simulating the surface waters of the Amazon River basin: impacts of new river geomorphic and flow parameterizations. Hydrol. Process. 22, 2542–2553. https://doi.org/10.1002/hyp.6850.

Coe, M.T., Costa, M.H., Soares-Filho, B.S., 2009. The influence of historical and potential future deforestation on the stream flow of the Amazon River – land surface processes and atmospheric feedbacks. J. Hydrol. 369, 165–174. https://doi.org/10.1016/j.jhydrol.2009.02.043.

Costa, M.H., Botta, A., Cardille, J.A., 2003. Effects of large-scale changes in land cover on the discharge of the Tocantins River, southeastern Amazonia. J. Hydrol. 283, 206–217. https://doi.org/10.1016/S0022-1694(03)00267-1.

da Rocha, M., de Assis, R.L., Piedade, M.T.F., Feitosa, Y.O., Householder, J.E., de Lobo, G., S., et al., 2019. Thirty years after Balbina Dam: diversity and floristic composition of the downstream floodplain forest, Central Amazon, Brazil. Ecohydrology 12, e2144. https://doi.org/10.1002/eco.2144.

Dag, O., Dolgun, A., Konar, N.M., 2018. Onewaytests: an R package for one-way tests in independent groups designs. R J. 10.

Dettinger, M.D., Diaz, H.F., 2000. Global characteristics of stream flow seasonality and variability. J. Hydrometeorol. 1, 289–310. https://doi.org/10.1175/1525-7541(2000)001<0289:GCOSFS>2.0.CO;2.

Dias, L.C.P., Macedo, M.N., Costa, M.H., Coe, M.T., Neill, C., 2015. Effects of land cover change on evapotranspiration and streamflow of small catchments in the upper Xingu River basin, Central Brazil. J. Hydrol. Reg. Stud. 4, 108–122. https://doi.org/10.1016/j.ejrh.2015.05.010.

Doria, C.R.C., Dutka-Gianelli, J., Brasil de Sousa, S.T., Chu, J., Garlock, T.M., 2020. Understanding impacts of dams on the small-scale fisheries of the Madeira River through the lens of the fisheries performance indicators. Mar. Policy 104261. https://doi.org/10.1016/j.marpol.2020.104261.

dos Santos, N.C.L., García-Berthou, E., Dias, J.D., Lopes, T.M., de Affonso, I.P., Severi, W., 2018. Cumulative ecological effects of a Neotropical reservoir cascade across multiple assemblages. Hydrobiologia 819, 77–91. https://doi.org/10.1007/s10750-018-3630-z.

Dubayah, R., Blair, J.B., Goetz, S., Fatoyinbo, L., Hansen, M., Healey, S., et al., 2020. The global ecosystem dynamics investigation: high-resolution laser ranging of the Earth's forests and topography. Sci. Remote Sens. 1, 100002. https://doi.org/10.1016/j.srs.2020.100002.

Ely, P., Fantin-Cruz, I., Tritico, H.M., Girard, P., Kaplan, D., 2020. Dam-induced hydrologic alterations in the Rivers feeding the pantanal. Fron. Environ. Sci. 8, 579031. https://doi.org/10.3389/fenvs.2020.579031.

Fearnside, P.M., 1999. Social impacts of Brazil's Tucuruí dam. Environ. Manag. 24, 483–495.

Ferreira, L.V., Cunha, D.A., Chaves, P.P., Matos, D.C.L., Parolin, P., 2013. Impacts of hydroelectric dams on alluvial riparian plant communities in eastern brazilian amazonian. An. Acad. Bras. Cienc. 85, 1013–1023. https://doi.org/10.1590/S0001-37652013000300012.

Florsheim, J.L., Mount, J.F., Chin, A., 2008. Bank erosion as a desirable attribute of Rivers. Bioscience 58, 519–529. https://doi.org/10.1641/B580608.

Fontana, L., Albuquerque, A.L.S., Brenner, M., Bonotto, D.M., Sabaris, T.P.P., Pires, M.A.F., et al., 2014. The eutrophication history of a tropical water supply reservoir in Brazil. J. Paleolimnol. 51, 29–43.

Fox, J., Ledgerwood, J., 1999. Dry-season flood-recession rice in the Mekong Delta: two thousand years of sustainable agriculture? Asian Perspect. 37–50.

Gergel, S.E., Carpenter, S.R., Stanley, E.H., 2005. Do dams and levees impact nitrogen cycling? Simulating the effects of flood alterations on floodplain denitrification. Glob. Chang. Biol. 11, 1352–1367. https://doi.org/10.1111/j.1365-2486.2005.00966.x.

Harris, I., Osborn, T.J., Jones, P., Lister, D., 2020. Version 4 of the CRU TS monthly high-resolution gridded multivariate climate dataset. Sci. Data 7. https://doi.org/10.1038/s41597-020-0453-3.

Horn, M.H., Correa, S.B., Parolin, P., Pollux, B.J.A., Anderson, J.T., Lucas, C., et al., 2011. Seed dispersal by fishes in tropical and temperate fresh waters: the growing evidence. Acta Oecol. 37, 561–577.

Horton, J.S., 1977. The development and perpetuation of the permanent tamarisk type in the phreatophyte zone of the Southwest. In: Johnson, R.R., Jones, D.A. (Eds.), Tech. Coords. Importance, Preservation and Management of Riparian Habitat: A Symposium. Gen. Tech. Rep. RM-43. US Department of Agriculture, Forest Service, Rocky Mountain Forest and Range Experiment Station, Fort Collins, CO, pp. 124–127.

Hupp, C.R., Pierce, A.R., Noe, G.B., 2009. Floodplain geomorphic processes and environmental impacts of human alteration along coastal plain rivers, USA. Wetlands 29, 413–429. https://doi.org/10.1672/08-169.1.

Jardine, T.D., Bond, N.R., Burford, M.A., Kennard, M.J., Ward, D.P., Bayliss, P., et al., 2015. Does flood rhythm drive ecosystem responses in tropical riverscapes? Ecology 96, 684–692. https://doi.org/10.1890/14-0991.1.

Jarvis, A., Rubiano, J.E., Nelson, A., Farrow, A., Mulligan, M., 2004. Practical Use of SRTM Data in the Tropics: Comparisons With Digital Elevation Models Generated Cartographic Data.

Junk, W.J., 2001. Sustainable use of the Amazon river floodplain: problems and possibilities. Aquat. Ecosyst. Health Manag. 4, 225–233. https://doi.org/10.1080/146349801753509122.

Junk, W.J., 2010. Amazonian Floodplain Forests: Ecophysiology, Biodiversity and Sustainable Management. Springer, Dordrecht [Netherlands] ; New York https://doi.org/10.1007/978-90-481-8725-6.

Junk, W.J., Bayley, P.B., Sparks, R.E., 1989. The flood pulse concept in river-floodplain systems. Can. Spec. Publ. Fish. Aquat. Sci. 106, 110–127.

Kingsford, R.T., 2000. Ecological impacts of dams, water diversions and river management on floodplain wetlands in Australia: impacts of dams and diversions on floodplain wetlands. Austral Ecol. 25, 109–127. https://doi.org/10.1046/j.1442-9993.2000.01036.x.

Klink, C.A., Machado, R.B., 2005. Conservation of the brazilian cerrado. Conserv. Biol. 19, 707–713. https://doi.org/10.1111/j.1523-1739.2005.00702.x.

Kozlowski, T.T., 2002. Physiological-ecological impacts of flooding on riparian forest ecosystems. Wetlands 22, 550–561. https://doi.org/10.1672/0277-5212(2002)022[0550:PEIOFO]2.0.CO;2.

Kubitzki, K., Ziburski, A., 1994. Seed dispersal in flood plain forests of Amazonia. Biotropica 26, 30. https://doi.org/10.2307/2389108.

Latrubesse, E.M., Arima, E.Y., Dunne, T., Park, E., Baker, V.R., D'Horta, F.M., et al., 2017. Damming the rivers of the Amazon basin. Nature 546, 363–369. https://doi.org/10.1038/nature22333.

Latrubesse, E.M., d'Horta, F.M., Ribas, C.C., Wittmann, F., Zuanon, J., Park, E., et al., 2020. Vulnerability of the biota in riverine and seasonally flooded habitats to damming of Amazonian rivers. Aquat. Conserv. Mar. Freshwat. Ecosyst. aqc.3424. https://doi.org/10.1002/aqc.3424.

Laufer, J., Marques, E.E., Athayde, S., Swanson, A.C., Zagallo, A.D.A., 2020. Rios, Terras e Culturas: aprendendo com o Sistema Socioecológico do Tocantins. Editora Fi, Porto Alegre https://doi.org/10.22350/9786587340197.

Lees, A.C., Peres, C.A., Fearnside, P.M., Schneider, M., Zuanon, J.A.S., 2016. Hydropower and the future of amazonian biodiversity. Biodivers. Conserv. 25, 451–466. https://doi.org/10.1007/s10531-016-1072-3.

Lehner, B., Grill, G., 2013. Global river hydrography and network routing: baseline data and new approaches to study the world's large river systems. Hydrol. Process. 27.

Leite Lima, M.A., Rosa Carvalho, A., Alexandre Nunes, M., Angelini, R., da Costa, Rodrigues, Doria, C., 2020. Declining fisheries and increasing prices: the economic cost of tropical rivers impoundment. Fish. Res. 221, 105399. https://doi.org/10.1016/j.fishres.2019.105399.

Li, X., Liu, J.P., Saito, Y., Nguyen, V.L., 2017. Recent evolution of the Mekong Delta and the impacts of dams. Earth Sci. Rev. 175, 1–17. https://doi.org/10.1016/j.earscirev.2017.10.008.

Lima, A.C., Agostinho, C.S., Sayanda, D., Pelicice, F.M., Soares, A.M.V.M., Monaghan, K.A., 2016. The rise and fall of fish diversity in a neotropical river after impoundment. Hydrobiologia 763, 207–221. https://doi.org/10.1007/s10750-015-2377-z.

Lima, J.E.F.W., dos Santos, P.M.C., de Carvalho, N.O., da Silva, E.M., 2003. Fluxo de sedimentos em suspensão na bacia Araguaia-Tocantins. ANEEL/ANA, Brasília, Brazil.

de Lobo, G.S., Wittmann, F., Piedade, M.T.F., 2019. Response of black-water floodplain (igapó) forests to flood pulse regulation in a dammed Amazonian river. For. Ecol. Manag. 434, 110–118. https://doi.org/10.1016/j.foreco.2018.12.001.

Lobón-Cerviá, J., Hess, L.L., Melack, J.M., Araujo-Lima, C.A.R.M., 2015. The importance of forest cover for fish richness and abundance on the Amazon floodplain. Hydrobiologia 750, 245–255. https://doi.org/10.1007/s10750-014-2040-0.

Magilligan, F.J., Nislow, K.H., 2005. Changes in hydrologic regime by dams. Geomorphology 71, 61–78. https://doi.org/10.1016/j.geomorph.2004.08.017.

Manyari, W.V., de Carvalho, O.A., 2007. Environmental considerations in energy planning for the Amazon region: downstream effects of dams. Energy Policy 35, 6526–6534. https://doi.org/10.1016/j.enpol.2007.07.031.

Marengo, J.A., Tomasella, J., Uvo, C.R., 1998. Trends in streamflow and rainfall in tropical South America: Amazonia, eastern Brazil, and northwestern Peru. J. Geophys. Res. Atmos. 103, 1775–1783. https://doi.org/10.1029/97JD02551.

McLeod, A.I., McLeod, M.A.I., 2015. Package 'Kendall.'. R Software, London, UK.

Moegenburg, S.M., 2006. Spatial and temporal variation in hydrochory in Amazonia floodplain forest. Biotropica 34, 606–612. https://doi.org/10.1111/j.1744-7429.2002.tb00581.x.
Mumba, M., Thompson, J.R., 2005. Hydrological and ecological impacts of dams on the Kafue flats floodplain system, southern Zambia. Phys. Chem. Earth 30, 442–447. https://doi.org/10.1016/j.pce.2005.06.009.
Naiman, R.J., Decamps, H., Pollock, M., 1993. The role of riparian corridors in maintaining regional biodiversity. Ecol. Appl. 3, 209–212. https://doi.org/10.2307/1941822.
Nardi, F., Annis, A., Baldassarre, G.Di, Vivoni, E.R., Grimaldi, S., 2019. GFPLAIN250m, a global high-resolution dataset of earth's floodplains. Sci. Data 6. https://doi.org/10.1038/sdata.2018.309.
Nilsson, C., Dynesius, M., 1994. Ecological effects of river regulation on mammals and birds: a review. Regul. Rivers Res. Manag. 9, 45–53. https://doi.org/10.1002/rrr.3450090105.
Oliveira-Filho, A.T., Ratter, J.A., 2002. Vegetation physiognomies and woody flora of the cerrado biome. In: Oliveira, P.S., Marquis, R.J. (Eds.), The Cerrados of Brazil: Ecology and Natural History of a Neotropical Savanna. Columbia University Press, New York, pp. 91–120.
Park, E., Latrubesse, E.M., 2017. The hydro-geomorphologic complexity of the lower Amazon River floodplain and hydrological connectivity assessed by remote sensing and field control. Remote Sens. Environ. 198, 321–332. https://doi.org/10.1016/j.rse.2017.06.021.
Parolin, P., 2012. Diversity of adaptations to flooding in trees of Amazonian floodplains. Pesquisas Bot. 63, 7–28.
Parolin, P., Lucas, C., Piedade, M.T.F., Wittmann, F., 2010. Drought responses of flood-tolerant trees in amazonian floodplains. Ann. Bot. 105, 129–139. https://doi.org/10.1093/aob/mcp258.
Parolin, P., Wittmann, F., 2010. Struggle in the flood: tree responses to flooding stress in four tropical floodplain systems. AoB Plants 2010. https://doi.org/10.1093/aobpla/plq003.
Pearson, A.J., Pizzuto, J.E., Vargas, R., 2016. Influence of run of river dams on floodplain sediments and carbon dynamics. Geoderma 272, 51–63. https://doi.org/10.1016/j.geoderma.2016.02.029.
Poff, N.L., Allan, J.D., Bain, M.B., Karr, J.R., Prestegaard, K.L., Richter, B.D., et al., 1997. The natural flow regime. Bioscience 47, 769–784. https://doi.org/10.2307/1313099.
Poff, N.L., Zimmerman, J.K.H., 2010. Ecological responses to altered flow regimes: a literature review to inform the science and management of environmental flows: review of altered flow regimes. Freshw. Biol. 55, 194–205. https://doi.org/10.1111/j.1365-2427.2009.02272.x.
Pokhrel, Y., Burbano, M., Roush, J., Kang, H., Sridhar, V., Hyndman, D.W., 2018. A review of the integrated effects of changing climate, land use, and dams on Mekong river hydrology. Water (Switzerland) 10, 266. https://doi.org/10.3390/w10030266.
R Core Team, 2020. R: A Language and Environment for Statistical Computing.
Ratter, J.A., Ribeiro, J.F., Bridgewater, S., 1997. The Brazilian cerrado vegetation and threats to its biodiversity. Ann. Bot. 80, 223–230. https://doi.org/10.1006/anbo.1997.0469.
Reily, P.W., Johnson, W.C., 1982. The effects of altered hydrologic regime on tree growth along the Missouri River in North Dakota. Can. J. Bot. 60, 2410–2422. https://doi.org/10.1139/b82-294.
Ribeiro, J.F., Walter, B.M.T., 1998. Fitofisionomias do bioma Cerrado. In: Sano, S.M., de Almeida, S.P. (Eds.), Cerrado: ambiente e flora. Embrapa-CPAC, Planaltina.
Rood, S.B., Mahoney, J.M., 1995. River damming and riparian cottonwoods along the Marias River, Montana. Rivers 5, 195–207.
Saint-Paul, U., Zuanon, J., Villacorta Correa, M.A., García, M., Fabré, N.N., Berger, U., et al., 2000. Fish communities in central amazonian white- and Blackwater floodplains. Environ. Biol. Fish 57, 235–250. https://doi.org/10.1023/A:1007699130333.
Shafroth, P.B., Stromberg, J.C., Patten, D.T., 2002. Riparian vegetation response to altered disturbance and stress regimes. Ecol. Appl. 12, 107–123.
Souza, C.M., Shimbo, J.Z., Rosa, M.R., Parente, L.L., Alencar, A.A., Rudorff, B.F.T., et al., 2020. Reconstructing three decades of land use and land cover changes in brazilian biomes with landsat archive and earth engine. Remote Sens. 12, 2735. https://doi.org/10.3390/RS12172735.
Swanson, A.C., Bohlman, S., 2021. Cumulative impacts of land cover change and dams on the land-water interface of the Tocantins River. Front. Environ. Sci. 9, 662904. https://doi.org/10.3389/fenvs.2021.662904.
Taylor, D.W., 1982. Eastern Sierra riparian vegetation: ecological effects of stream diversion. Mono Basin Research Group Contribution.
Thomas, J., Joseph, S., Thrivikramji, K.P., Arunkumar, K.S., 2014. Sensitivity of digital elevation models: the scenario from two tropical mountain river basins of the Western Ghats, India. Geosci. Front. 5, 893–909. https://doi.org/10.1016/j.gsf.2013.12.008.
Timpe, K., Kaplan, D., 2017. The changing hydrology of a dammed Amazon. Sci. Adv. 3, e1700611. https://doi.org/10.1126/sciadv.1700611.
Trancoso, R., Carneiro Filho, A., Tomasella, J., Schietti, J., Forsberg, B.R., Miller, R.P., 2009. Deforestation and conservation in major watersheds of the brazilian Amazon. Environ. Conserv. 36, 277–288. https://doi.org/10.1017/S0376892909990373.
Tundisi, J.G., Matsumura-Tundisi, T., Calijuri, M.C., 1993. Limnology and management of reservoirs in Brazil. Comparative Reservoir Limnology and Water Quality Management, pp. 25–55 https://doi.org/10.1007/978-94-017-1096-1_2.
van Oorschot, M., Kleinhans, M., Buijse, T., Geerling, G., Middelkoop, H., 2018. Combined effects of climate change and dam construction on riverine ecosystems. Ecol. Eng. 120, 329–344.
Wang, Y., Wang, D., Lewis, Q.W., Wu, J., Huang, F., 2017. A framework to assess the cumulative impacts of dams on hydrological regime: a case study of the Yangtze River. Hydrol. Process. 31, 3045–3055.
Welcomme, R.L., Halls, A., 2004. Dependence of tropical river fisheries on flow. Proceedings of the Second International Symposium on the Management of Large Rivers for Fisheries (RAP Publication 2004/16. Food and Agriculture Organization of the United Nations), pp. 267–283.
Wittmann, F., Schöngart, J., Junk, W.J., 2010. Phytogeography, species diversity, community structure and dynamics of central Amazonian floodplain forests. Amazonian Floodplain Forests. Springer, pp. 61–102 https://doi.org/10.1007/978-90-481-8725-6_4.
Wood, S., Wood, M.S., 2015. Package 'mgcv.' R Package Version 1, p. 29.
World Comission on Dams, 2000. Dams and Development: A New Framework for Decision-making: The Report of the World Commission on Dams. Earthscan.
Zamora-Arroyo, F., Nagler, P.L., Briggs, M., Radtke, D., Rodriquez, H., Garcia, J., 2001. Regeneration of native trees in response to flood releases from the United States into the delta of the Colorado River, Mexico. in. J. Arid Environ., 49–64 https://doi.org/10.1006/jare.2001.0835 (Academic Press).
Zhang, Y., Zheng, H., Herron, N., Liu, X., Wang, Z., Chiew, F.H.S., et al., 2019. A framework estimating cumulative impact of damming on downstream water availability. J. Hydrol. 575, 612–627.